

Flavin Mononucleotide as a Corrosion Inhibitor for Hot Rolled Steel in Hydrochloric Acid

Shaily M. Bholal*, Gurmeet Singh², Brajendra Mishra¹

¹ Department of Metallurgical & Materials Engineering, Colorado School of Mines, Golden, CO 80401 USA

² Department of Chemistry, University of Delhi, Delhi, 110007 INDIA

*E-mail: malhotra.shaily@gmail.com

Received: 14 February 2013 / Accepted: 20 March 2013 / Published: 1 April 2013

FMN was investigated as a green corrosion inhibitor for hot rolled steel in 1M HCl using potentiodynamic polarization, temperature kinetics studies and quantum chemical calculations. The inhibition efficiency increases with increase in concentration as well as temperature. Adsorption is favored at higher temperatures due to chemisorption and the adsorption follows Frumkin's isotherm. The mechanism of adsorption has been proposed from the analysis of kinetic parameters such as ΔG_{ads}° and E_a . Quantum chemical analysis has been performed on FMN and the charge density maps and various optimized molecular parameters have been illustrated with an explanation on the involvement of charge centres in the adsorption process.

Keywords: FMN, corrosion inhibitor, eco-friendly, HCl, chemisorption

1. INTRODUCTION

Corrosion of iron and steel is one of the fundamental corrosion problems in the industry today. Acid solutions are widely used in applications involving metallic materials such as acid pickling, industrial acid cleaning, acid descaling and oil well acidizing. Heterocyclic compounds display potential properties for use as corrosion inhibitors due to the presence of nitrogen, oxygen and sulphur in their ring structure [1-3]. In addition, planarity due to the presence of π electrons and lone pairs of electrons on the heteroatoms contribute to their efficiency as inhibitors. In the recent past, there has been an increased interest in the use of environmental friendly corrosion inhibitors for metals in various media [4-5]. The aim of the present investigation is to study the corrosion inhibition behavior of flavin mononucleotide, which is a green inhibitor, on the corrosion of hot rolled steel in 1M HCl.

Flavin mononucleotide (7, 8-dimethyl-10-ribityl-isoalloxazine-5' phosphate monosodium salt dihydrate) is a phosphate monosodium dihydrated salt of Vitamin B₂ (Riboflavin). It consists of a heterocyclic isoalloxazine ring attached to the sugar alcohol, ribitol, which is derived from a D(-) pentose sugar (ribose) that contains three antisymmetric carbons and a phosphate monosodium salt (Figure 1).

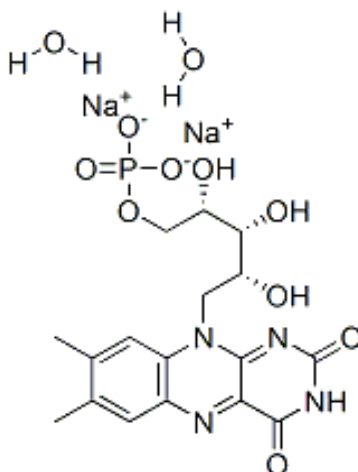


Figure 1. Structure of FMN

2. EXPERIMENTAL

A 569 hot rolled steel of composition (0.02-0.15% C, 0.6% Mn, 0.03% P, 0.035% S, 0.2% Cu, 0.2% Ni, 0.15% Cr, 0.06% Mo, 0.008% V, 0.008% Nb, 0.025% Ti and remaining Fe) following ASTM Standard [6] was used for the present investigation. Corrosion studies were performed in 1M HCl solution in the absence and presence of various concentrations of flavin mononucleotide (FMN) such as 2×10^{-3} , 10^{-3} , 10^{-4} , 10^{-5} and 10^{-6} M at five different temperatures namely, 293, 303, 313, 323 and 333 K. A three electrode system with steel as the working electrode, saturated calomel electrode as the reference electrode and platinum wire as the counter electrode were used for the study. Prior to experimentation, the steel specimens were finished upto 600 grit emery paper and washed with double distilled water and acetone.

Potentiodynamic polarization experiments were conducted using a PAR Potentiostat 273A. The data was generated by polarizing the steel specimens from -500 mV vs. OCP (open circuit potential) upto a final potential of 1 V vs. SCE at a scan rate of 1 mV/s. The immersion time was chosen as 1 hour for all the experiments. Each test was run in duplicate to verify the reproducibility and the average values are reported.

For the quantum chemical calculations, HyperChem Standard 5.1 for windows (Hypercube Inc. Canada) [7-8] was used to create the initial geometry of FMN. The geometry of the inhibitor was fully optimized by using the MM⁺ (Molecular Mechanics) and then through AM1 (Austin Model 1) with Polak Ribierre gradient method and the calculations for the various molecular parameters were

performed through UHF method. The convergence limit for optimization with respect to the total energy was taken as 0.1 kcal.

3. RESULTS AND DISCUSSION

Figure 2 shows the potentiodynamic polarization curves for steel in 1M HCl in the absence and presence of various concentrations of FMN and Table 1 gives the corresponding polarization parameters. The inhibition efficiency of FMN was calculated using the following equation:

$$I\% = [I_{\text{corr (1M HCl)}} - I_{\text{corr (FMN)}}] \times 100 / I_{\text{corr (1M HCl)}} \quad (1)$$

It is clear from Table 1 that the inhibition efficiency of FMN increases with increase with the inhibitor concentration. Moreover, the addition of FMN to 1M HCl shifts the E_{corr} to slightly negative values, suggesting that FMN acts preferentially as a cathodic inhibitor. This can also be observed from the polarization curves in Figure 1, where FMN appears to affect the cathodic reaction more than the anodic reaction.

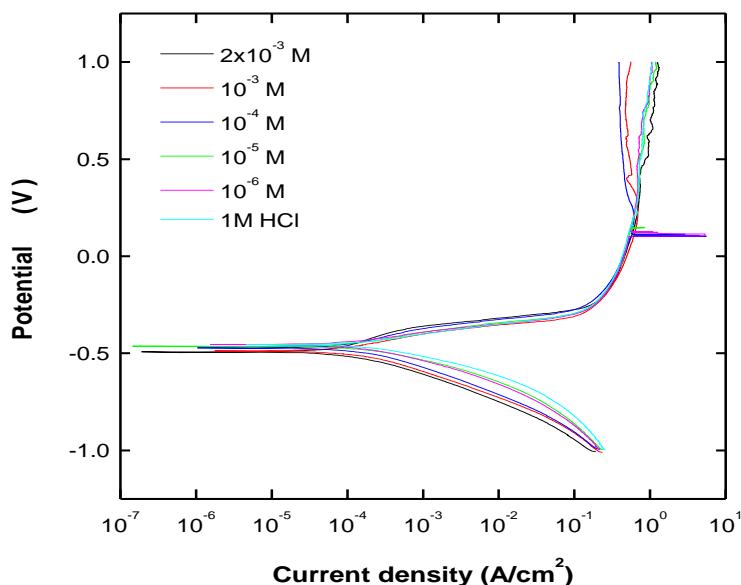


Figure 2. Potentiodynamic polarization curves of steel in the absence and presence of different concentrations of FMN in 1M HCl at 293 K

Table 1. Polarization parameters for steel in the absence and presence of different concentrations of FMN in 1M HCl at 293 K

C_{FMN} (M)	$-E_{\text{corr}}$ (mV)	I_{corr} (mA/cm ²)	$-b_c$ (mV/decade)	b_a (mV/decade)	I%
2×10^{-3}	446.45	0.199	142.51	40.75	59.45
10^{-3}	432.93	0.224	163.71	44.19	54.34
10^{-4}	430.97	0.247	135.89	44.92	49.53
10^{-5}	425.05	0.410	134.34	42.15	16.36
10^{-6}	414.51	0.450	116.91	49.12	8.34
Blank	410.17	0.490	118.44	49.43	-

Figure 3 displays the variation between surface coverage, θ (%I/100) and logarithm of inhibitor concentration. The curve obeys Frumkin's isotherm, with a characteristic S shape [9-10].

The Frumkin equation is:

$$\theta/1-\theta e^{-2a\theta} = K_{\text{ads}}C \quad (2)$$

where a is a molecular interaction parameter depending on the molecular interaction in the adsorption layer and on the degree of heterogeneity of the surface, C is the concentration of the inhibitor and K_{ads} is the equilibrium constant of the adsorption reaction. The standard adsorption free energy change ($\Delta G^{\circ}_{\text{ads}}$) was obtained by the relation:

$$\Delta G^{\circ}_{\text{ads}} = -2.303 RT \log 55.5 K_{\text{ads}} \quad (3)$$

where, 55.5 is the concentration of water in solution expressed in M.

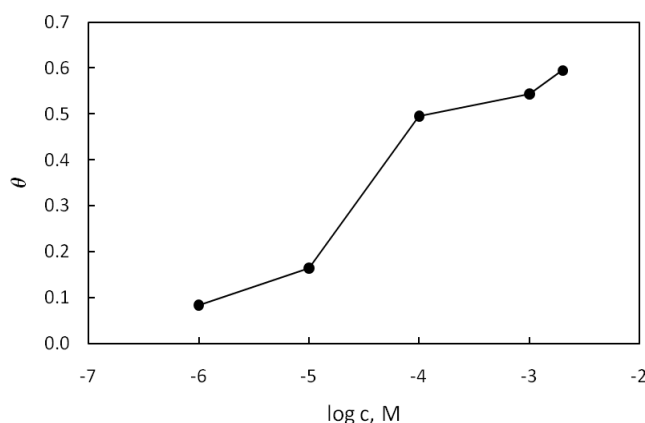


Figure 3. Variation of surface coverage with logarithmic concentration of FMN in 1M HCl at 293 K

The Frumkin's isotherm fitted best amongst various other isotherms investigated, with a mean R^2 value of 0.91 for all temperatures. The $\Delta G^{\circ}_{\text{ads}}$ values were calculated to be -38.43, -50.68, -54.92, -57.78 and -58.17 kJ mol^{-1} respectively at 293, 303, 313, 323 and 333 K. The values of $\Delta G^{\circ}_{\text{ads}}$ obtained are negative, which suggests that the adsorption of FMN is a spontaneous process [11-12]. Generally, values of $\Delta G^{\circ}_{\text{ads}}$ around -20 kJ mol^{-1} or lower are consistent with electrostatic interaction between the charged molecules and the charged metal (physisorption) and those around -40 kJ mol^{-1} or higher involve charge sharing or transfer from the inhibitor molecules to the metal surface to form a coordinate bond (chemisorption) [13-14]. The absolute value of $\Delta G^{\circ}_{\text{ads}}$ increases with increase in temperature, indicating that the adsorption becomes favorable with increasing temperatures [15]. The $\Delta G^{\circ}_{\text{ads}}$ value at 293 K appears to show a comprehensive adsorption mechanism involving both physisorption and chemisorption whereas at all higher temperatures, chemisorption favours. Chemisorption can take place on the steel surface by the interaction between the π electrons of the heterocyclic ring and the lone pair of electrons on the heteroatoms and the vacant low energy d orbitals of the Fe surface atoms. Physisorption, which might take place in addition to chemisorption at low

temperatures, could result from the electrostatic interaction between the protonated FMN molecule in acid solution (at the basic nitrogen and oxygen centers) and the negatively charged steel surface. Moreover, Fe²⁺ ions are known to chelate FMN [16] and the chelate formed might get physically adsorbed on the steel surface by means of electrostatic adsorption. At higher temperatures, where only chemisorption is observed, the chelate might get easily desorbed due to its increased solubility with increased solution agitation.

Table 2 illustrates the effect of temperature on the corrosion of steel in 1M HCl in the absence and presence of 2x10⁻³ M FMN. The corrosion current density of steel in 1M HCl increases with temperature, both in the absence and presence of FMN. The inhibition efficiency increases or remains equally effective with increase in temperature. The effective activation energy for the corrosion process was calculated from the Arrhenius equation:

$$\log I_{\text{corr}} = \log A - E_a/2.303RT \tag{4}$$

where, A is the Arrhenius factor and E_a is the effective activation energy.

Figure 4 shows the Arrhenius plots displaying the variation between logarithm of corrosion current density and inverse of temperature for 1M HCl in the absence and presence of 2x10⁻³ M FMN. The E_a values were obtained from the slopes of the best fit lines and have been listed in Table 3. The E_a values for various concentrations of FMN are lower than E_a for acid, further confirming the role of chemisorption in the adsorption process [17-19].

Table 2. Effect of temperature on the corrosion of steel in 1M HCl and 1M HCl+2x10⁻³ M FMN

T (K)	I _{corr} (mA/cm ²) (1M HCl)	I _{corr} (mA/cm ²) (2x10 ⁻³ M FMN)	I% (2x10 ⁻³ M FMN)
293	0.490	0.199	59.4
303	1.828	0.205	88.7
313	8.492	0.572	93.2
323	11.87	2.206	81.4
333	81.53	4.971	93.9

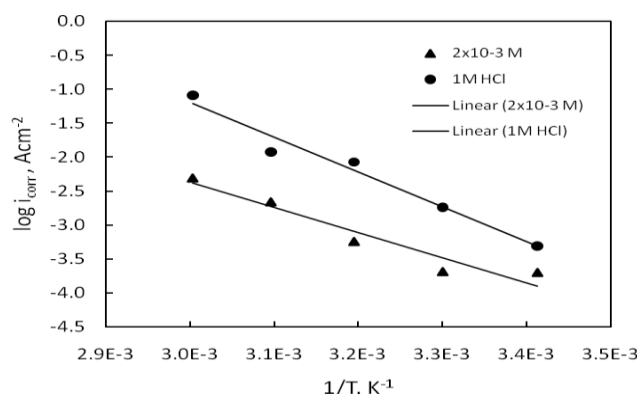


Figure 4. Arrhenius plots for steel in 1M HCl in the absence and presence of 2x10⁻³ M FMN

Table 3. Effective activation energy values for steel in 1M HCl in the absence and presence of various concentrations of FMN

Concentration (M)	E_a (kJ mol ⁻¹)	R^2
2×10^{-3}	70.92	0.9261
10^{-3}	77.64	0.9483
10^{-4}	84.12	0.9838
10^{-5}	78.37	0.9597
10^{-6}	92.94	0.9630
HCl	98.06	0.9694

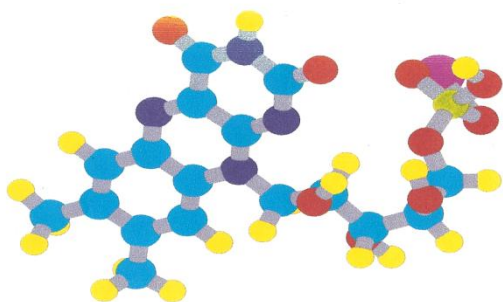
Quantum chemical calculations are a powerful tool for determining the efficacy of a corrosion inhibitor by means of various molecular parameters and the geometry of a molecule [7,20]. Fig. 5a shows the optimized geometry of the inhibitor as a ball and stick model and the various optimized parameters calculated are given in Table 4. Figures 5 (b-e) show the 3-D isosurfaces of total charged density HOMO and LUMO, electrostatic potential mapped on to the 3-D charged density isosurface and charge density map for active sites of FMN. In the charge density maps of HOMO, LUMO and electrostatic potential, green colour indicates positive electron density and pink colour indicates negative electron density.

In the charge density maps of HOMO and LUMO in Figure 5b and 5c, it can be observed that the charges are localized around the isoalloxazine ring, which is the heterocyclic moiety consisting of π electrons of the ring structure and the lone pairs on N and O imparting negative charge density to the molecule. The negative charge centers on the molecule can chemisorb by forming $d\pi$ - $p\pi$ coordinate bonds with Fe. The planarity of the isoalloxazine ring, as seen in Figure 5a, favors the adsorption of FMN on the surface of steel. FMN shows a relatively higher value of E_{HOMO} and a lower value of E_{LUMO} as compared with some other organic heterocyclic inhibitors [20], which favors the adsorption of FMN with the metal surface.

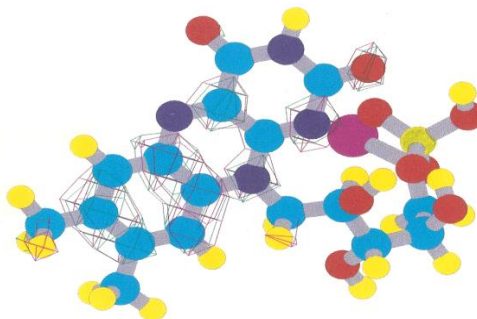
Table 4. Optimised AM1 parameters for the inhibitors using Hyperchem 5.1

No. of electrons	184
Total Energy (kcal/mol)	-145331.75
Energy of HOMO (eV)	-9.335
Energy of LUMO (eV)	-1.396
$E_{\text{LUMO}}-E_{\text{HOMO}}$ (eV)	7.939
Binding Energy (kcal/mol)	-5458.21
Electronic Energy (kcal/mol)	-1151734.16
Core-Core Interaction (kcal/mol)	1006402.408
Heat of Formation (kcal/mol)	-421.59
Dipole Moment (Debye)	11.921

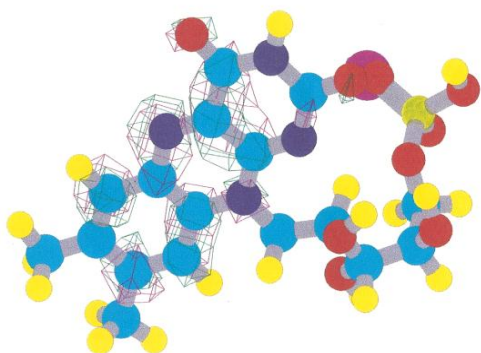
As E_{HOMO} is associated with the electron donating ability of the molecule, high values of E_{HOMO} indicate the ability of the molecule to donate electrons to the acceptor molecule with low energy and empty molecular orbital. The electronic configuration of Fe is $1s^2 2s^2 2p^6 3s^2 3p^6 4s^2 3d^6$. The incomplete 3d orbital of Fe could bond with HOMO of FMN while the filled 4s orbital could interact with LUMO of FMN. The negative binding energy of FMN in Table 4 shows that the molecule is very stable. Very high value of dipole moment suggests that it is a polar compound and can easily donate π electrons forming strong $d\pi$ - $p\pi$ bonding.



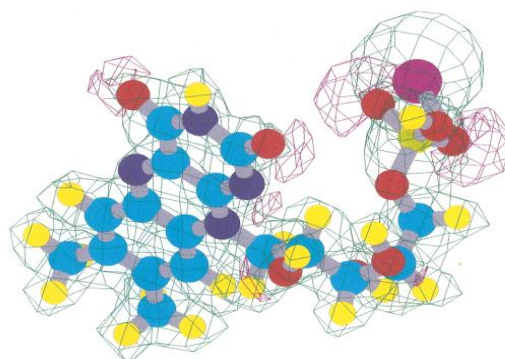
(a). Ball & stick model of FMN



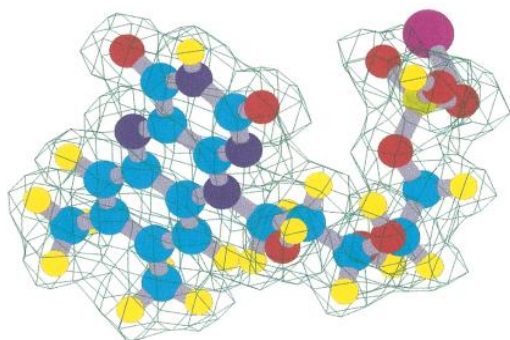
(b). 3-D isosurface of total charge density of HOMO



(c). 3-D isosurface of total charge density of LUMO



(d). Electrostatic potential mapped on to the 3-D charge density isosurface



(e). Charge density map for active sites of FMN

Figure 5. (a-e) - 3-D isosurfaces of FMN

4. CONCLUSIONS

1. FMN is a potential inhibitor for corrosion of hot rolled steel in acidic medium.
2. The inhibition efficiency of FMN increases with both concentration and temperature.
3. The inhibitor follows Frumkin's isotherm with negative values of $\Delta G_{\text{ads}}^{\circ}$, which signifies that the adsorption is a spontaneous process. High $\Delta G_{\text{ads}}^{\circ}$ values indicate that the adsorption takes place by chemisorption at all temperatures except at the lowest temperature, where comprehensive adsorption exists.
4. The E_a values for various concentrations of FMN are lower than E_a for acid, further confirming the role of chemisorption in the adsorption process.
5. Quantum chemical analysis suggests that adsorption of FMN is mainly concentrated around the isoalloxazine ring.

References

1. M.A. Quraishi and R. Sardar, *Corrosion* 58, (2002) 2
2. S.L. Granese, B.M. Rosales, C. Oviedo, J.O. Zerbino, *Corrosion Science* 33, (1992) 1493
3. S.N. Banerjee, S. Mishra, *Corrosion* 45, (1989) 780
4. A.A. Elhosary, R.M. Saleh. in: J.M. Costa, A.D. Mercer (Ed.), *Progress in the Understanding and Prevention of Corrosion*, Institute of Materials, (1983), 923
5. A.Y. El-Etre, *Corrosion Science* 45, (2003) 2485
6. ASTM Standard A 1011/A 1011M - 09a, ASTM International, USA
7. G. Bereket, C. Ogretir, C. Ozsahin, *Journal of Molecular Structure: Theochem.* 663, (2003) 39-46
8. M. Lagrenee, B. Mernari, N. Chaibi, M. Traisnel, H. Vezin, F. Bentiss, *Corros. Sci.* 43(5), (2001) 951-962
9. N. Frumkin, *J. Phys. Chem.* 116, (1925) 466
10. A.S. Fouda, A.A. Al-Sarawy, E.E. El-Kator, *Desalination* 201, (2006) 1-13
11. M. Elachouri, M.S. Hajji, M. Salem, S. Kertit, J. Aride, R. Coudert, E. Essassi, *Corrosion* 52, (1996) 103
12. S.A. Ali, H.A. Al-Muallem, M.T. Saeed, S. U. Rahman, *Corrosion Science* 50, (2008) 664
13. K.F. Khaled, *Electrochimica Acta* 53, (2008) 3484
14. M. Kaddouri, N. Cheriaa, R. Souane, M. Bouklah, A. Aouniti, R. Abidi, B. Hammouti, J. Vicens, *J. Appl. Electrochem.* 38, (2008) 1253
15. Ehteram A. Noor, Aisha H. Al-Moubaraki, *Materials Chemistry and Physics* 110, (2008) 145-154
16. F. Funk, J. P. Lenders, Robert R. Crichton, Walter Schneider, *European Journal of Biochemistry* 152(1), (1985) 167-172
17. K. Tebbji, N. Faska, A. Tounsi, H. Oudda, M. Benkaddour, B. Hammouti, *Mater. Chem. Phys.* 106, (2007) 260
18. L. Herrag, A. Chetouani, S. Elkadiri, B. Hammouti, A. Aouniti, *Port. Electrochim. Acta* 26, (2008) 211
19. A. Popova, *Corrosion Science* 49, (2007) 2144
20. G. Bereket, C. Ogretir, C. Ozsahin, *J. Mol. Struct: Theochem* 663, (2004) 173